

# Effect of Functional Group and Surface Charge of PEG and Dextran-Coated USPIO as a Contrast Agent in MRI on Relaxivity Constant

Nastaran Najafian<sup>1,2</sup> · Saeed Shanehsazzadeh<sup>3</sup> ·  
Farzaneh Hajesmaeelzadeh<sup>1,2</sup> · Afsaneh Lahooti<sup>2</sup> ·  
Cordula Gruettner<sup>4</sup> · Mohammad Ali Oghabian<sup>1,2</sup>

Received: 2 March 2015 / Revised: 7 March 2015 / Published online: 26 March 2015  
© Springer-Verlag Wien 2015

**Abstract** The challenges in molecular imaging are focused on the development of novel contrast agents with much lower relaxation times. Ultrasmall superparamagnetic iron oxide nanoparticles known as USPIO have been used for a variety of applications such as imaging of cancer, apoptosis, and hyperthermia providing higher signal changes based on  $T_2^*$  weighted susceptibility effects. Although many studies had been performed on USPIO there is still a lack of data on the effects of the physicochemical properties of these nanoparticles (NP) such as hydrodynamic size, surface charge and type of functional groups, which may alter the relaxivity of these NPs. The aim of this study was to evaluate the effect of different functional groups and surface charges of PEGylated and dextran-coated NPs on their magnetic properties. All relaxometry studies were performed using a 3-T magnetic resonance imaging. Our results showed that the impact of charge on magnetic properties is much higher than that of coating thickness. In this respect, particles with positive surface charges showed higher  $r_2/r_1$  ratios.

---

✉ Mohammad Ali Oghabian  
oghabian@sina.tums.ac.ir

- <sup>1</sup> Biomolecular Imaging Analysis Group (BIAG), Research Center for Molecular and Cellular Imaging (RCMCI), Tehran University of Medical Sciences, Tehran, Iran
- <sup>2</sup> Department of Medical Physics and Biomedical Engineering, Faculty of Medicine, Tehran University of Medical Science, Tehran, Iran
- <sup>3</sup> Radiation Application Research School, Nuclear Science and Technology Research Institute (NSTRI), Tehran, Iran
- <sup>4</sup> Micromod Partikeltechnologie GmbH, Friedrich-Barnewitz-Str. 4, 18119 Rostock, Germany

## 1 Introduction

Early detection of many diseases especially cancer is very important for the treatment efficiency. Diagnostic devices such as magnetic resonance imaging (MRI), positron emission tomography (PET), and single photon emission computed tomography (SPECT) are used for this purpose. MRI shows advantages over the other methods due to its high spatial resolution and non-invasive imaging [1–4]. Due to the low sensitivity and specificity of MRI compared to nuclear medicine devices (e.g., PET or SPECT), which is the main disadvantage of this method, the need of contrast agents as a key solution is increasing [5–7]. The increasing importance of the emerging field of magnetic nanoparticles (MNPs) as a contrast agent in MRI is due to their higher relaxivity and their magnetic susceptibilities [8–10]. Ultrasmall superparamagnetic iron oxide nanoparticles (USPIO) are used as  $T_2$  weighted contrast agent (a negative contrast agent) in MRI because of their high magnetic moment [11, 12]. Surface coatings including dextran, citrate and polyethylene glycol (PEG) provide stability and improved biocompatibility of the MNPs. They can alter their relaxivity, biodistribution and stability by their physicochemical properties such as size and type of iron oxide crystals, hydrodynamic size, surface charge and functional groups [13]. The ability of a contrast agent to enhance the proton relaxation rate is defined in terms of its relaxivity [14]:

$$R_{1,2} = 1/T_{1,2} = R_{1,2}^0 + r_{1,2} C \quad (1)$$

where  $R_{1,2}^0$  is the relaxation rate of ( $R_1$  or  $R_2$ ) without the presence of the contrast agent.  $C$  is the concentration of the nanoparticles in molar of the contrast agent and  $r_{1,2}$  is the relaxivity constants ( $T_1$ - and  $T_2$ -relaxivity) of the agent. The unit of  $r_1$  and  $r_2$  is  $\text{mM}^{-1} \text{s}^{-1}$ .

Extensive studies have been done on USPIO and demonstrate the key role of surface charge in the changing of accumulation and half-life of nanoparticle and contrast of MRI [9, 11, 15, 16]. Amiri et al. [17] investigated USPIO with variation in the thickness and functional group type (surface charges) of the dextran surface coating with and without protein corona. At the absence of the protein corona, the relaxivity of positively charged MNPs was higher than for plain USPIOs and negatively charged USPIOs [17]. Although, several studies were carried out on magnetic properties of NPs there is still a lack of quantitative data about the effects of functional groups on the relaxation times of the NPs. Therefore, in this study we examine the physicochemical properties and compare different charges and functional groups ( $\text{NH}_2$ ,  $\text{COOH}$ , plain) of some commercial USPIO nanoparticles, which were coated with dextran and PEGylated dextran. The relaxivity data of the different MNPs were determined in the water phantom for the development of MRI contrast agents.

## 2 Materials and Methods

The MNPs were provided from micromod Partikeltechnologie GmbH (Germany) with product codes (79-00-201, 77-01-201, 79-02-201) for dextran-coated MNPs and (79-54-102, 79-55-201, 79-56-201) for corresponding PEGylated MNPs. The full information on the particles is provided in Table 1.

**Table 1** Description of the employed MNP samples

Sample No.	Product code	Product name	Surface	Ø (nm)	Concentration (mg/ml)
1	79-02-201	Nanomag <sup>®</sup> -D-SPIO <sup>a</sup>	COOH	20	5
2	77-01-201	Nanomag <sup>®</sup> -CLD- SPIO <sup>b</sup>	NH <sub>2</sub>	20	5
3	79-00-201	Nanomag <sup>®</sup> -D- SPIO	Plain	20	5
4	79-55-201	Nanomag <sup>®</sup> -D- SPIO	PEG-NH <sub>2</sub>	20	5
5	79-56-201	Nanomag <sup>®</sup> -D- SPIO	PEG-COOH	20	5
6	79-54-201	Nanomag <sup>®</sup> -D- SPIO	PEG 300	20	5

<sup>a</sup> Dextran iron oxide composite particles (suspension in water)

<sup>b</sup> Cross-linked dextran iron oxide composite particles (suspension in water)

## 2.1 Nanoparticles Characterization

The characterizations of the MNPs were performed with different methods. The core size and morphology of dextran-coated USPIOs were investigated by transmission electron microscope (TEM, Philips CM100, Netherlands). After the micrographs were obtained, the Clemex Vision PE 4 software performed image analysis. The core size of the iron oxide crystals in the 20 nm MNPs was measured previously with a mean diameter of 7–10 nm [9, 18, 19]. The hydrodynamic particle size was investigated by photon correlation spectroscopy (PCS). The PCS measurements were performed with a Malvern Zetasizer Nano ZS-90 (Malvern Instruments Ltd., Worcestershire, UK). Inductively coupled plasma atomic emission spectroscopy (ICP-AES, Varian-Liberty, 150 AX Turbo, USA) was performed to determine the iron concentrations of the particle suspensions after digesting the samples with boiling HNO<sub>3</sub> [20, 21].

## 2.2 MRI Measurements

MRI of samples (in test tubes) with various iron concentrations (0.02, 0.01, 0.005, 0.0025, 0.00125 and 0.000625 mg/ml) was performed using a 3-T MR scanner (Siemens, Magnetom Trio) and a standard circularly polarized head coil (Clinical MR Solutions, Brookfield, WI, USA). All MNPs were placed in a water-containing plastic container at room temperature to avoid susceptibility artifacts from the surrounding air in the scans. For quantitative data analysis, the images were transferred to a local workstation, and the  $T_1$  and  $T_2$  maps were calculated assuming mono-exponential signal decay [22, 23].  $T_1$  images were attained using eight SE images with a fixed TE of 12 ms, and TR values of 200, 400, 1000, 2000, 3000, and 4000 ms. For the  $T_1$  calculation, a non-linear function least-square curve fitting on a pixel-by-pixel basis was used. Signal intensity is expressed in Eq. (2):

$$SI_{(\text{pixel } xy)} = S_{0(\text{pixel } xy)} \left[ 1 - e^{-\text{TR}/T_{1(\text{pixel } xy)}} \right] \quad (2)$$

For  $T_2$  maps, four SE images with a fixed TR of 3000 ms, and TE values of 24, 36, 48 and 60 ms were taken [6, 7]. The signal intensity for each pixel as a function of time is expressed in Eq. (3):

$$SI_{(\text{pixel } xy)} = S_{0(\text{pixel } xy)} \left[ e^{-TE/T_{2(\text{pixel } xy)}} \right] \quad (3)$$

Special care was taken to analyze only data points with signal intensities significantly above the noise level\_ENREF\_31. Spin-spin or transverse relaxation time ( $T_2$ )-weighted spin echo (SE) images were acquired using variable repetition time (TR) and echo (TE) times of TR/TE = 256/16 ms, and TR/TE = 3000/64 ms, and then analyzed qualitatively [24]. All sequences were acquired with a field of view of  $160 \times 160$  mm, a matrix of  $256 \times 196$  pixels, and slide thickness of 3 mm. Initially, the signal intensities of all test tubes with contrast medium at different iron concentrations were assessed visually [8].

### 3 Results

Figures. 1 and 2 represent the TEM data and hydrodynamic sizes of the nanoparticles, respectively. As seen in Fig. 1, the average of the iron oxide crystal core size is  $8.86 \pm 1.61$  nm. The PCS measurements demonstrate that the hydrodynamic size of MNPs varies in the range of 67–111 nm (Fig. 2). For the

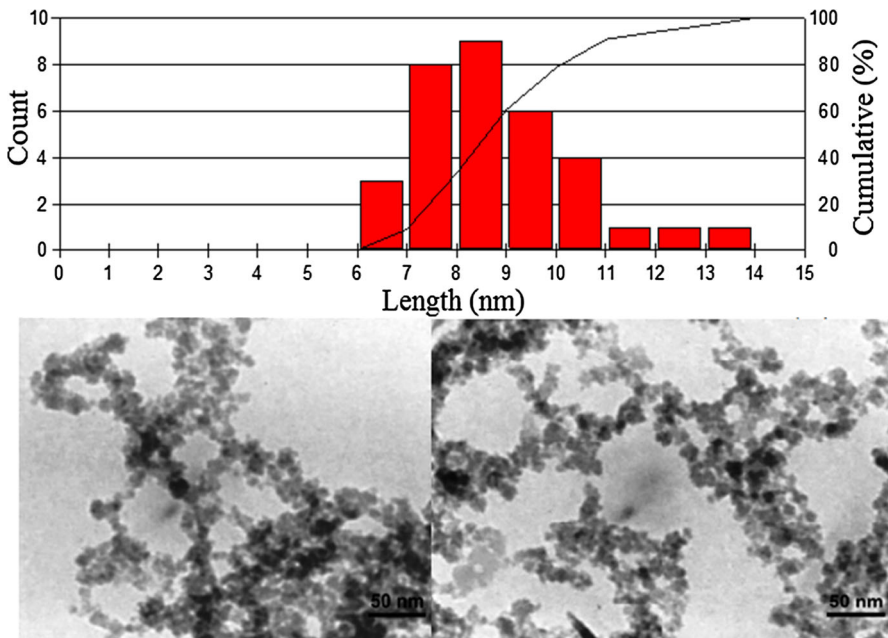


**Fig. 1** TEM image of the NPs (inset shows the  $8.86 \pm 1.61$  nm iron oxide crystal core size of the bare USPIO)

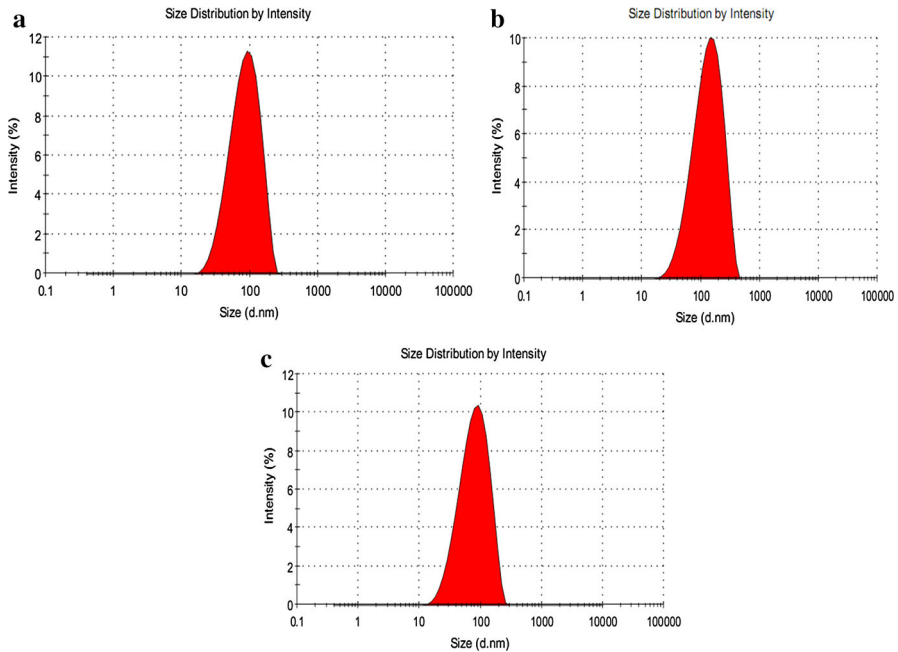


**Fig. 2** PCS data of dextran-coated MNPs: **a** plain MNP with a  $z$ -average of 74 nm. **b**  $\text{NH}_2$  functionalized MNPs with a  $z$ -average of 111 nm. **c**  $\text{COOH}$  functionalized MNPs with a  $z$ -average of 67 nm

dextran as well as the corresponding PEGylated dextran-coated MNPs the hydrodynamic diameters increase in dependence on the type of functional groups on the surface in the order of  $\text{COOH} < \text{plain} < \text{NH}_2$  (Table 2).

The mean relaxivity of the NPs is represented in Table 2. Results showed that  $r_2/r_1$  ratio of PEGylated NPs with  $\text{NH}_2$  is 54 and 24 % higher than NPs with plain and  $\text{COOH}$  functional group, respectively. On the other hand, the  $r_2/r_1$  ratio for dextran NPs with Amine group is 73 and 101 % higher than NPs with plain and  $\text{COOH}$  functional group, respectively. The  $R_2$  and  $R_1$  of the NPs among different iron concentrations are shown in Fig. 3. The  $R_{2,1}$  ( $1/T_{2,1}$ ) was plotted versus different concentration, and the slope of the line gives relaxivity ( $r_{2,1}$ ).

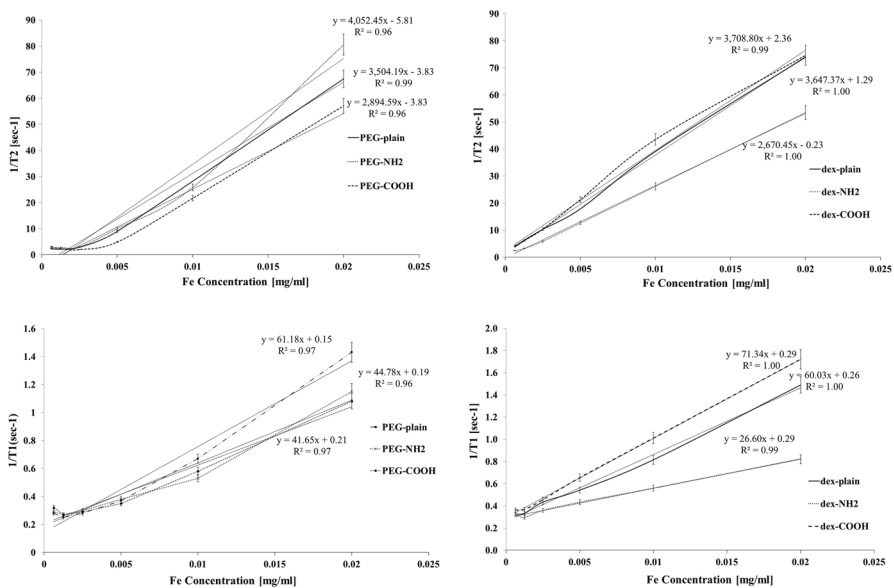
The  $r_2/r_1$  ratios for nanoparticles were represented in Fig. 4. Results showed the  $r_2/r_1$  ratio for  $\text{NH}_2$  is higher in both dextran group and PEG group.

## 4 Discussions

The influence of the physicochemical properties of MNPs with the same core particle and different surface modifications on their relaxivity data was studied. As presented in Fig. 4, there are significant differences in both coating groups in terms of  $r_2/r_1$  ratios among different surface charges. The  $r_2/r_1$  ratios increase in the order of functional groups for  $\text{COOH} < \text{plain} < \text{NH}_2$ . In the same order, the

**Table 2** Mean relaxivity values of MNPs coated with dextran and PEGylated dextran together with the hydrodynamic diameters

Samples	Hydrodynamic size (nm)	$r_2$ ( $\text{mm}^{-1} \text{s}^{-1}$ )	$r_1$ ( $\text{mm}^{-1} \text{s}^{-1}$ )	$r_2/r_1$
PEG-plain	74.34	$15.34 \pm 0.01$	$0.25 \pm 0.02$	$60.64 \pm 1.43$
PEG-NH <sub>2</sub>	93.96	$17.47 \pm 0.01$	$0.19 \pm 0.00$	$93.44 \pm 1.49$
PEG-COOH	59.45	$12.42 \pm 0.11$	$0.17 \pm 0.01$	$75.30 \pm 2.51$
dex-plain	74	$15.74 \pm 0.01$	$0.26 \pm 0.01$	$59.73 \pm 1.38$
dex-NH <sub>2</sub>	111	$11.50 \pm 0.01$	$0.11 \pm 0.00$	$103.61 \pm 1.02$
dex-COOH	67.37	$15.93 \pm 0.05$	$0.31 \pm 0.02$	$51.52 \pm 3.31$

**Fig. 3** Relaxivity data of PEGylated and corresponding dextran-coated MNPs in dependence on the iron concentration. The *slope* of the lines gives the relaxivities

hydrodynamic diameters of the MNPs increase (Table 2). These findings could be due to two reasons. In relation to the results of Amiri et al. [17], we also found higher relaxivities for the NPs with amino groups. The other potential reason is the differences in hydrodynamic size of these MNPs. Duan et al. [25] showed that by increasing the hydrophilicity, the  $r_2$  values increase. Their results were in accordance to our findings. Larsen et al. [26] showed for PEG coated NPs that larger hydrodynamic sizes resulted in higher  $r_2$  values which is similar to our results for PEGylated NPs (Table 2). The type of coating (PEG-dextran or dextran) did not affect the  $r_2/r_1$  ratio of the plain particles. For positively charged MNPs (i.e., MNPs with NH<sub>2</sub> groups), the  $r_2/r_1$  ratio and the hydrodynamic size were increased from the

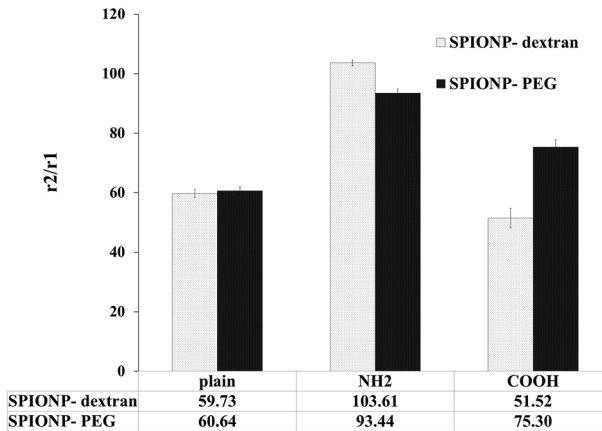


**Fig. 4** The  $r_2/r_1$  ratio for the different types of MNPs

PEG-dextran to the dextran surface. Whereas for negatively charged MNPs (i.e., MNPs with COOH groups), the  $r_2/r_1$  ratio was decreased from the PEG-dextran to the dextran surface at increasing particle size.

Our results showed that the  $r_2/r_1$  ratios of particles with the same functional groups were much more dependent on the surface charge than on the hydrodynamic size of the MNPs. This should be due to higher quota of charge effects in relaxometry compared to hydrodynamic size increments. Although further studies should be carried in order to confirm these results.

## 5 Conclusions

In this study, we evaluated the effect of surface charges of MNPs on their relaxivities to obtain information for an optimal surface design of MNPs as contrast agent in MRI. MNPs with the same core particle, but different surface modifications were studied. Particles with a dextran surface as well as a PEG-dextran surface were investigated with a plain surface and with amino or carboxylic acid groups on the surface. These different surface modifications influenced the hydrodynamic particle diameter of the MNPs. Therefore, we evaluated both hydrodynamic size and charge effects on the magnetic properties of dextran-coated and PEGylated MNPs. Our results showed that the impact of surface charge on magnetic properties of MNPs is much higher than that of their hydrodynamic size for dextran and PEG-dextran-coated particles. MNPs with a positive surface charge (with amino groups) had higher  $r_2/r_1$  ratios than corresponding MNPs with a plain or negatively charged surface (COOH groups). Essentially the  $r_2/r_1$  ratios increase with increasing hydrodynamic particle diameters.

**Acknowledgments** We thank Micromod Company for their supports in terms of providing nanoparticles and the quantitative analysis of the particles. Council of Research of Tehran University of Medical Sciences (TUMS), Tehran, Iran, supported this work.

**Conflict of Interest** The authors declare that they have no conflict of interest.

## References

1. A. Akbarzadeh, M. Samiei, S. Davaran, *Nanoscale Res. Lett.* **7**, 1–13 (2012)
2. S.M. Cromer Berman, P. Walczak, J.W. Bulte, *WIREs Nanomed. Nanobiotechnol.* **3**, 343–355 (2011)
3. K. Luo, J. Tian, G. Liu, J. Sun, C. Xia, H. Tang, L. Lin, T. Miao, X. Zhao, F. Gao, J. *Nanosci. Nanotechnol.* **10**, 540–548 (2010)
4. J. Xie, G. Liu, H.S. Eden, H. Ai, X. Chen, *Acc. Chem. Res.* **44**, 883–892 (2011)
5. M. Amanlou, S.D. Siadat, S.E.S. Ebrahimi, A. Alavi, M.R. Aghasadeghi, M.S. Ardestani, S. Shanehsaz, M. Ghorbani, B. Mehravi, M.S. Alavidjeh, *Int. J. Nanomed.* **6**, 747–763 (2011)
6. R. Jahanbakhsh, F. Atyabi, S. Shanehsazzadeh, Z. Sobhani, M. Adeli, R. Dinarvand, *DARU* **21**, 53–62 (2013)
7. H. Omid, M.A. Oghabian, R. Ahmadi, N. Shahbazi, H.R.M. Hosseini, S. Shanehsazzadeh, R.N. Zangeneh, *BBA Gen. Subj.* **1840**, 428–433 (2014)
8. M.A. Oghabian, N. Gharehaghaji, A. Masoudi, S. Shanehsazzadeh, R. Ahmadi, R.F. Majidi, H.R.M. Hosseini, *Adv. Sci. Eng. Med.* **5**, 37–45 (2013)
9. S. Shanehsazzadeh, M.A. Oghabian, F.J. Daha, M. Amanlou, B.J. Allen, J. *Radioanal. Nucl. Chem.* **295**, 1517–1523 (2013)
10. I. Coroiu, A. Darabont, D.E. Demco, *Appl. Magn. Reson.* **15**, 531–538 (1998)
11. S. Shanehsazzadeh, A. Lahooti, *Nucl. Med. Biol.* **41**, 625 (2014)
12. S. Shanehsazzadeh, M.A. Oghabian, A. Lahooti, M. Abdollahi, S.A. Haeri, M. Amanlou, F.J. Daha, B.J. Allen, *Nucl. Med. Commun.* **34**, 915–925 (2013)
13. C. Corot, P. Robert, J.M. Idée, M. Port, *Adv. Drug Deliv. Rev.* **58**, 1471–1504 (2006)
14. R.E. Hendrick, E. Mark Haacke, *J. Magn. Reson. Imaging* **3**, 137–148 (1993)
15. S. Shanehsazzadeh, M. Oghabian, B. Allen, M. Amanlou, A. Masoudi, F. Daha, *J. Med. Phys.* **38**, 34–40 (2013)
16. G. Gambarota, H.W.M. van Laarhoven, M. Philippens, W.J.M. Peeters, P. Rijken, A. van der Kogel, C.J.A. Punt, A. Heerschap, *Appl. Magn. Reson.* **38**, 349–360 (2010)
17. H. Amiri, L. Bordonali, A. Lascialfari, S. Wan, M.P. Monopoli, I. Lynch, S. Laurent, M. Mahmoudi, *Nanoscale* **5**, 8656–8665 (2013)
18. S. Shanehsazzadeh, M. Oghabian, B. Allen, M. Amanlou, F.J. Daha, *World Congress on Medical Physics and Biomedical Engineering, Beijing, China May 26–31, 2012* (Springer, Heidelberg, 2012), pp. 2204–2207
19. S.N. Tabatabaei, J. Lapointe, S. Martel, in *IEEE/RSJ International Conference on Intelligent Robots and Systems. IROS 2009*, pp. 546–551
20. H. Wang, J. Wang, X. Deng, H. Sun, Z. Shi, Z. Gu, Y. Liu, Y. Zhao, *J. Nanosci. Nanotechnol.* **4**, 1019–1024 (2004)
21. F. Scherer, M. Anton, U. Schillinger, J. Henke, C. Bergemann, A. Kruger, B. Gansbacher, C. Plank, *Gene Ther.* **9**, 102–109 (2002)
22. S. Shanehsazzadeh, C. Gruettner, A. Lahooti, M. Mahmoudi, B.J. Allen, M. Ghavami, F.J. Daha, M.A. Oghabian, *Contrast Media Mol. Imaging* (2014). doi:10.1002/cmml.1627
23. A. Yilmaz, M. Yurdakoc, J. Bernarding, H.M. Vieth, J. Braun, A. Yurt, *Appl. Magn. Reson.* **22**, 11–22 (2002)
24. A. Yilmaz, H. Budak, R. Longo, *Appl. Magn. Reson.* **14**, 51–58 (1998)
25. H. Duan, M. Kuang, X. Wang, Y.A. Wang, H. Mao, S. Nie, *J. Phys. Chem. C* **112**, 8127–8131 (2008)
26. E.K. Larsen, T. Nielsen, T. Wittenborn, L.M. Rydtoft, A.R. Lokanathan, L. Hansen, L. Ostergaard, P. Kingshott, K.A. Howard, F. Besenbacher, N.C. Nielsen, J. Kjems, *Nanoscale* **4**, 2352–2361 (2012)